

Anisotropy of electron-phonon scattering in gold

C. A. Steele* and R. G. Goodrich

Department of Physics and Astronomy, Louisiana State University, Baton Rouge, Louisiana 70803

(Received 23 June 1981)

The temperature dependences of radio-frequency size-effect signals have been measured and used to obtain a functional form for the anisotropy of the electron-phonon interaction for electrons on the Fermi surface of gold. The signals were observed at 23 different orientations. The temperature behavior of these signals gives the orbitally averaged values for the strength of the electron scattering by phonons. The data from these orbits, repeated for different thicknesses of the samples, were used with a mathematical inversion scheme to establish a functional form for point values of the electron-phonon interaction $\nu(\vec{k})$ over the Fermi surface of gold.

INTRODUCTION

The parallel field radio-frequency size effect (RFSE) is a valuable tool for measuring the electron-phonon (e - p) scattering rates of electrons on the Fermi surface (FS) of metals. The RFSE for many years has been used to determine FS dimensions, and in recent years has proved to be the only reliable method by which e - p scattering rates for orbits on the FS of metals can be determined.¹ Experimentally, the RFSE involves the detection of changes in the surface impedance of a thin single crystal slab of metal placed in a magnetic field applied parallel to the crystal surface. At magnetic field values, such that an extremal cyclotron orbit of an electron on the FS exactly spans the sample thickness, an abrupt change in the surface impedance of the sample is observed. The magnitude of the magnetic field at which the change occurs is directly proportional to an extremal dimension of the FS. The magnitude of the change in impedance is proportional to the rate at which scattering events occur along the orbit.

In this paper we will not be concerned with measurements of the precise values of the FS dimensions, but rather with the scattering events which the electrons encounter. The amplitude of the parallel field RFSE is proportional to the algebraic sum of the probabilities of the electrons being able to travel across the sample without being scattered. That is,

$$A = A_0 \sum_{n=1}^{\infty} \exp(-n\pi\bar{\nu}_{\text{eff}}/\Omega) \\ = A_0 [\exp(\pi\bar{\nu}_{\text{eff}}/\Omega) - 1]^{-1},$$

where n counts the number of traverses of the electron across the sample thickness, $\bar{\nu}_{\text{eff}}$ is the average total scattering frequency around the orbit, and $\Omega = eB/m^*C$ is the cyclotron frequency for the orbit of effective mass m^* at the magnetic field B .

The total scattering frequency is composed of several parts: $\bar{\nu}_I$, the temperature-independent scattering frequency due to impurities and dislocations; $\bar{\nu}_{ep}$, the e - p scattering frequency which is proportional to the temperature cubed T^3 ; and $\bar{\nu}_{ee}$, the electron-electron (e - e) scattering frequency which should vary as T^2 . We explicitly assume Matthiessen's Rule and write

$$\bar{\nu}_{\text{eff}} = \bar{\nu}_I + \bar{\nu}_{ee} + \bar{\nu}_{ep} \\ = \bar{\nu}_I + \alpha T^2 + \gamma T^3,$$

where all of the coefficients are the average value experienced by an electron around its cyclotron orbit. With data from a sufficient number of orbits it is then desirable to invert the data to obtain values for $\nu_I(\vec{k})$, $\alpha(\vec{k})$, and $\gamma(\vec{k})$ for each point on the FS. In gold the dominant temperature-dependent term is the e - p interaction and we have used a series of symmetrized Fourier coefficients to invert the values of γ to obtain $\gamma(\vec{k})$. This process has been described in detail by Johnson and Goodrich (JG).²

EXPERIMENT

Sample preparation

A single crystal ingot was grown from Comino 69's pure gold. Considerable care was taken to ensure that the gold suffered minimum contamination during the crystal growth. A graphite cruci-

ble was made from Union Carbide ECV Grade stock which has low ash content and small particle size. A quite lengthy purification procedure for the graphite was followed to eliminate metal and organic impurities. This procedure is to soak in aqua-regia, rinse in distilled and deionized water, dry in air at 80 °C, bake in vacuum at 1100 °C, bake in a partial atmosphere of chlorine gas at 1100 °C, and finally heat it to 1400 °C until a vacuum of 10^{-6} Torr is achieved.

The crystal-growing apparatus is of the Bridgman type using rf induction heating of the graphite crucible placed on a water cooled cold finger. We found it unnecessary to encourage controlled solidification from the bottom (nearest the cold finger) by moving the rf coil. Instead a sufficient temperature gradient down the crucible was maintained by placing the rf coil near the top of the crucible. The crystal growth procedure began by heating the crucible containing the gold pellets to 780 °C in a vacuum of 10^{-5} Torr in order to drive off any contaminants on the surface of the gold. The rf power was then turned down and the gold allowed to cool. Helium gas from liquid-helium boiloff was passed through a LN₂ temperature charcoal trap and introduced into the evacuated growing chamber to a pressure of 700 mm Hg. The helium atmosphere is necessary to suppress the deposition of gold onto the inside surface of the quartz vacuum chamber, rendering it opaque. The rf power was gradually applied until the gold was 200 °C above its melting temperature of 1064 °C. The melt was then cooled at a rate of 14 °C every ten minutes with a temperature gradient of 30 °C being maintained along the crystal length of approximately 18 mm. The resultant single crystal, when at room temperature, was free of the crucible.

The resistance ratio of the ingot as grown was measured using the Bean technique and gave a ratio of $\rho_{300}/\rho_{4.2} \simeq 2700$. An anneal in a partial atmosphere of pure oxygen was attempted in order to improve the return. The ingot was left in a furnace at 1000 °C with oxygen gas at a pressure of 2×10^{-4} Torr for 38 h and cooled at 50 °C per hour in a vacuum of 10^{-5} Torr. This treatment only increased the resistance ratio to 3300. Since gold does not react with air at elevated temperatures, a final treatment was a simple anneal in air at 1000 °C for 30 h. This produced our highest measured value for the resistance ratio for the ingot of 4500.

Preparation of the samples from the crystal proved to be rather troublesome due to the chemi-

cal inertness of this metal. The experiment required a thick sample to be prepared and for it to be thinned down in stages with data taken after each thinning. An additional requirement was that the samples be thinned without causing any structural damage, the requirement being that ν_I , the temperature-independent scattering frequency should be constant for all thicknesses of any one sample.

To begin with the ingot was crystallographically oriented and a slice cut using spark erosion. A 0.13-mm diameter beryllium-copper traveling wire was used as a cutting tool with a spark energy of 40 μ J and a spark current of 25 mA. Each cut through the crystal took approximately 7 h. The cut surfaces were mechanically polished and the damaged surface layer was removed by an electropolish. The electropolish solution consisted of 7.8 gm KCN, 0.78 gm KFI, 0.78 gm K₂CO₃, 31.3 cc glycerine, and 4.7 cc of water. The solution was heated to 85 °C and a current density of approximately 800 mA/cm² at 12 v removed the gold at a rate of 40 μ m/min from each side. Typically 60 μ m was removed from each surface. It was not possible to remove any more of the metal without causing the surfaces to become rippled. This polish results in extremely bright surfaces. After polishing the samples were reannealed in air at 975 °C for 12 h. Samples prepared in this manner have strong RFSE signals.

Once a complete set of measurements was completed on one sample, it was thinned down by employing the chemical polishing technique described by Young and Wilson.³ The polishing solution consists of 1 part concentrated HNO₃, 3 parts concentrated HCl, and 3 parts phosphoric acid. A rotating disk acid polisher was used and this solution was dripped onto the cloth-covered polishing wheel. This procedure enabled several hundred microns to be removed and kept the surfaces flat and parallel. The finish was not as bright as that produced by the electropolish and small deviations from a planar surface were indicated by distortion in reflected images.

Samples

Three successful samples were prepared. They were labeled Au1, Au4, and Au5. The first sample, Au1, was the only one that was chemically thinned for thickness-dependent measurements. Data were obtained on this sample at thicknesses

of 1.051, 0.692, and 0.527 mm. Signals were not observed in thick samples with $\hat{n}||[100]$, therefore, no thickness dependence of the signals for this orientation could be measured. A summary of the orientation and thickness on which measurements were made is given in Table I.

Apparatus

The RFSE signals were detected using the 5-MHz limiting oscillator described by Ruthruff and Goodrich,⁴ and the overall field modulation detection system is described in Ref. 5. Temperature measurements were made with a carbon resistor which was calibrated in place over the temperature range used to the superconducting transition temperature of rhenium, indium, lead, and niobium as well as the boiling and lambda points of liquid helium. All resistance measurements on the thermometer were made with an ac conductance bridge which injected less than 10^{-6} W into the sample chamber. Data were recorded on an x - y recorder and signal amplitudes were read directly from the graph paper. The mean value of the amplitude of at least three tracings was taken as a datum for each measurement point.

RESULTS

In the discussion which follows we frequently refer to the amplitude of the signals and we mean by this natural logarithm of this quantity. These amplitudes are proportional to $\exp(\pi\bar{v}_{\text{eff}}/\Omega)$, therefore it is natural to discuss them in terms of their natural logarithms. The amplitude of the RFSE signals which we observed in gold obeyed a cubic temperature behavior for all samples in the temperature range of 3.7–8 K. For some of the measured orbits the amplitude behavior below 3.7 K

deviated from a T^3 dependence. All of the data reported here are from measurements of the amplitudes of the RFSE signals taken above 3.7 K where the e - p scattering and its anisotropy are dominant and can be obtained from the gradients of the \ln of the amplitudes vs T^3 .

A set of measurements was taken on samples 1, 2, and 3 for the magnet angle 70° from $[110]$. The temperature behavior of the signals for all three thicknesses was cubic over the full experimental temperature range. This enabled us to determine the orbitally averaged e - p interaction \bar{v}_{ep} and the temperature-independent scattering rate \bar{v}_I . The iterative model developed by Kimball, Adams, and Goodrich⁶ (KAG) was employed to do this. In this parametrized model different values of \bar{v}_{ep} and \bar{v}_I are used until the calculated gradients for the temperature dependence for each thickness agree closely with the experimental values. The KAG model involves five possible adjustable parameters: v_{ep} , v_I , Θ_D , Q , and α where Θ_D is an effective Debye temperature, Q is proportional to the total surface impedance of the sample, and α is a scattering effectiveness parameter. The effective Debye temperature is important only when the FS dimensions are on the order of phonon wave vector and in gold this is not the case. Hence, Θ_D was set equal to its measured value of 170 K and not adjusted. The value of the parameter Q is important for thin samples when an orbiting electron spends an appreciable portion of its orbit in the skin depth. For the present relatively thick sample results we set $Q=0$ and did not adjust it. Finally the effectiveness parameter $\tilde{\alpha}$ was set to the value given in KAG of $\Theta_D\delta$, where δ is the skin depth as determined from the RFSE linewidth, and not adjusted further. Thus, only the two parameters \bar{v}_{ep} and \bar{v}_I were used to fit all of the experimental data.

The best fit for \vec{B} 70° from $[110]$ was obtained for $\bar{v}_{ep} = 18.51 \times 10^6 \text{ K}^3 \text{ sec}^{-1}$ and $\bar{v}_I = 3.44 \times 10^9 \text{ sec}^{-1}$. Further checks showed that $\bar{v}_I(\vec{k})$

TABLE I. Data on gold samples used in the measurements.

Sample number	Orientation of normal to sample	Room temperature thickness (mm)
1	[110]	1.051
2	[110]	0.692
3	[110]	0.527
4	[110]	0.345
5	[100]	0.246

was isotropic within our experimental uncertainty and that for sample number 1 we were in the single pass limit. Isotropy in $\bar{\nu}_I(\vec{k})$ also has been observed in Dingle temperature measurements on gold.⁷ All other measurements to determine $\bar{\nu}_{ep}(\vec{k})$ in the [110] orientation were made on Au1. The value of $\bar{\nu}_I$ for the $\hat{n}||[100]$ sample was different due to defects introduced during the initial sample preparation. In order to obtain this value in Au5 where we are not in the single pass limit we used the fact that an identical orbit is observed for $\vec{B}||[100]$ in the [110] plane and for $\vec{B}||[100]$ in the [100] plane. We took the value of $\bar{\nu}_{ep}$ from the $\hat{n}||[110]$ sample for this orbit and adjusted $\bar{\nu}_I$ to give the experimental gradient for Au5. The value of $\bar{\nu}_I$ found for Au5 is $3.73 \times 10^9 \text{ sec}^{-1}$.

The values of $\bar{\nu}_{ep}$ which we obtained over 23 different orbits on the FS of gold are given in Table

II. All of these orbits except 23 are closed, maximum caliper orbits originating from the belly region of the FS. Many other extremal orbits, both open and closed, are observed in the RFSE measurements, but they are not included in the analysis. Orbit 23 is unique in that it does not originate from the belly region of the FS. The signal was observed in sample 4 with $\vec{B}||[111]$ and has a caliper value of $0.182k_F$ where k_F is the free electron radius of the Fermi sphere for gold. The signal is weak compared to other observed signals and moves rapidly to higher fields with decreasing amplitude as the field is rotated from [111]. This signal originates from an orbit around the neck of the FS where it contacts the Brillouin zone boundary. We were not able to determine a value of $\bar{\nu}_I$ for this orbit since it is not observed in the thicker samples. If a value of $\bar{\nu}_I = 3.7 \times 10^9 \text{ sec}^{-1}$ as mea-

TABLE II. Magnetic field direction, effective masses, and electron-phonon scattering rates for orbits on the Fermi surface of gold.

Orbit No.	θ (from [100])		m^*/m_0^a	γ ($10^6 \text{ sec}^{-1} \text{ K}^{-3}$)
1	0	$\hat{n} [100]$	1.142	14.98
2	5		1.123	12.98
3	10		1.094	12.81
4	15		1.071	12.91
5	20		1.060	14.62
6	25		1.072	16.46
7	30		1.130	19.38
8	32		1.199	22.64
9	32.4		1.224	28.72
		$\hat{n} [110]$		
1	0		1.142	14.98
10	5		1.122	16.21
11	10		1.083	17.06
12	15		1.050	16.04
13	20		1.038	15.19
14	23		1.053	14.03
15	24		1.068	14.71
16	48		1.086	12.28
17	50		1.074	11.22
18	55		1.065	10.73
19	60		1.072	12.44
20	65		1.095	15.49
21	70		1.156	18.51
22	72	1.218	21.15	
23	neck orbit 54.7	0.280	71.7	

^aEffective masses calculated from the model of Ref. 10.

sured in other thin samples is assumed, then $\bar{v}_{ep} = 72 \times 10^6 \text{ K}^3 \text{ sec}^{-1}$ is obtained for this neck orbit with $\vec{B}_j || [111]$.

We wish to interject here a note concerning the observation of this neck orbit in RFSE measurements. The FS's of copper, silver, and gold are nearly identical and while the neck orbit was observed and used in the e - p scattering analysis of copper Gantmakher and Gasparov⁸ and is observed here in gold, two independent studies on silver, Gasparov⁹ and JG, failed to observe this orbit. We have made extensive additional measurements on thin samples of silver to determine the reason for the lack of observation of signals due to this orbit. The answer lies in a coincidence concerning the FS caliper values for silver compared to copper and gold. In $\hat{n} || [110]$ samples for fields along [111] there exists in all three metals an extremal open orbit which travels through the neck region and over the belly region of the FS. As the field is rotated away from [111] this orbit becomes an extended-zone closed orbit. The RFSE signal to which it corresponds measures the difference in the extent of the neck and belly regions along [110]. In silver these signals occur at fields which overlap the fields at which signals from neck orbits should occur and are much stronger signals due to the fact that electrons on these orbits spend a large fraction of time on the belly region of the FS where the scattering rate is much smaller than on the necks. In copper and gold the FS dimensions are such that these two signals are separated in field and can be independently observed.

Finally, we note that for some orientations of the magnetic field the amplitudes deviate from a T^3 behavior in the lowest temperature ranges. The present data are not sufficiently accurate to determine in a quantitative manner what the functional form of this behavior is, but it is tending toward a lower power of T . Measurements at temperatures less than 1 K will have to be made before an analysis can be performed.

ANALYSIS

The results were analyzed in the manner described by Gantmakher and Gasparov.⁸ In brief form the object is to obtain an analytical representation for the anisotropy in $v_{ep}(\vec{k})$ for points on the FS. It is expressed as a series:

$$v_{ep}(\vec{k}) = T^3 \sum_{i=1}^t w_i F_i(\vec{k}),$$

where the w_i are coefficients which are determined by fitting the expression to the experimental data and the $F_i(\vec{k})$'s are the functions having the cubic symmetry of the lattice. These functions are a symmetrized Fourier series,

$$F_{lmn}(\vec{k}) = \sum_{lmn} \cos(lak_x/2) \cos(mak_y/2) \\ \times \cos(nak_z/2),$$

where $l^2 + m^2 + n^2 = 0, 2, 4, \dots$ for the face centered lattice of gold, $a = 4.0652A$, and the sum is over permutations of x, y , and z .

The orbital averaged measured value of \bar{v}_{ep} for the j th orbit is related to the point values on the orbit $v_{ep}(\vec{k})$ by

$$\bar{v}_{ep_j} = \frac{\hbar}{2\pi m_j^*} \oint_j \left[\frac{v(\vec{k})}{V_1} \right] d\vec{k},$$

where m_j^* is the effective mass of the orbit and V_1 is the projection of the velocity of the electrons onto the plane of the orbit. These two parameters were calculated from the model for the FS of gold given by Lengeler *et al.*¹⁰ Thus the weighted sums to be fit to the experimental data are

$$\frac{\bar{v}_{ep_j}}{T^3} = \sum_{i=1}^t a_{ij} w_i, \quad (1)$$

where

$$a_{ij} = \frac{\hbar}{2\pi m_j^*} \oint_j \frac{F_i(\vec{k}) d\vec{k}}{V_1(\vec{k})}.$$

The first step is to evaluate the a_{ij} since they are functions of known quantities. There are then j equations for the j measured orbits given by Eq. 1 where the only unknowns are the w_i . Provided t is less than j , then this represents an overdetermined set of equations and the values of the w_i can be determined by a generalized least-squares method.

We have achieved the best fit to all of the present data with a modified form of the above procedures. The form we have used was proposed in JG for silver and uses the fact that the scattering frequencies in the noble metals, in general, are proportional to the k -space dimension of the FS where they are being evaluated. Thus, we multiply each $F_i(\vec{k})$ by the dimensionless quantity $(|\vec{k}| - k_{min}) / k_{min}$, where k_{min} is treated as an adjustable parameter having a value less than $|\vec{k}|$

at any point on the FS. We find the best fit using four terms in the expansion plus a value of $k_{\min} = 1.105 \times 10^8 \text{ cm}^{-1}$. The overall fit to the data is better using this form than it is using up to five

terms in the expansion alone at which point oscillations in the fit began to set in. With this value the 22 central belly orbits are fit with a rms error of 8.9% by the following function:

$$\bar{\nu}^*/T^3 = (59.14 + 57.11F_{110} - 18.00F_{200} - 41.47F_{211})[(|\vec{k}| - k_{\min})/k_{\min}] \times 10^6 \text{ sec}^{-1} \text{ K}^{-3}. \quad (2)$$

A plot of this function in symmetry planes is shown in Fig. 1. The function is very steep in the neck region and gives a value of $\bar{\nu}^*/T^3 = 49.5 \times 10^6 \text{ sec}^{-1} \text{ K}^{-3}$ at the zone boundary to within the accuracy of the FS dimensions given by Halse.¹¹ Our measured value of $\bar{\nu}/T^3$ for the neck orbit with $\vec{B}||[111]$ is about 50% higher than the calculated values at two points on the neck orbit. However, slight changes in the FS dimensions from the Halse values can make large changes in the calculated scattering frequencies in this region.

The values of $\bar{\nu}_{ep}$ which have been used in this analysis are the energy averaged values determined from the slopes of the data. When the scattering frequencies are evaluated at the Fermi energy⁶ it is found that $\bar{\nu}_{ep}(\text{expt})/\bar{\nu}_{ep}(\text{Fermi energy}) = 1.24$. The free electron value for this ratio is 12/7.¹²

SUMMARY

We have observed the temperature dependence of the amplitude of RFSE signals for 22 parallel-field extremal belly orbits and the neck orbit on the FS of gold. From these measurements we have extracted the average electron-phonon collision frequency $\bar{\nu}_{ep}/T^3$ for each orbit. A functional form for the anisotropic e - p scattering frequency $\bar{\nu}^*(\vec{k})$ was derived from the data through an inversion procedure. The function derived in this manner fits the belly orbit data with a rms error of 8.9% and is given in Eq. (2). At the lowest temperature investigated the data deviate from the temperature dependence expected for e - p scattering but no interpretation of the limited data exhibiting this behavior can be given.

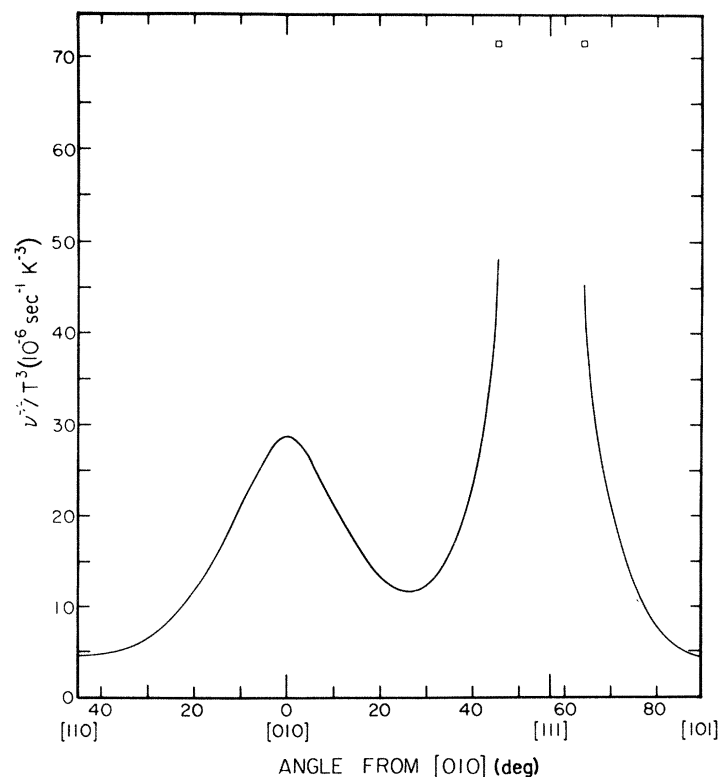


FIG. 1. Anisotropy of the electron-phonon scattering frequency in symmetry planes for gold. The squares near the [111] direction represent the measured values for the neck orbit.

ACKNOWLEDGMENT

This work was supported in part by NSF Grant No. DMR-8009826.

*Present address: Laser-Scan Laboratories, Cambridge, CB4 4BO England.

¹D. K. Wagner and R. Bowers, *Adv. Phys.* 27, 651 (1978).

²P. B. Johnson and R. G. Goodrich, *Phys. Rev. B* 14, 3286 (1976).

³R. W. Young, Jr. and T. R. Wilson, *Rev. Sci. Instrum.* 32, 559 (1961).

⁴T. L. Ruthruff and R. G. Goodrich, *J. Phys. E* 12, 94 (1979).

⁵T. L. Ruthruff, Ph.D. Dissertation, Louisiana State University, 1978 (unpublished).

⁶J. C. Kimball, L. W. Adams, and R. G. Goodrich, *Phys. Rev. B* 19, 2905 (1979).

⁷B. Lengeler, *Phys. Rev. B* 15, 5504 (1977).

⁸V. F. Gantmakher and V. A. Gasparov, *Zh. Eksp. Teor. Fiz.* 64, 1712 (1973) [*Sov. Phys. — JETP* 37, 864 (1973)].

⁹V. A. Gasparov, *Zh. Eksp. Teor. Fiz.* 68, 2259 (1975) [*Sov. Phys. — JETP* 41, 1129 (1976)].

¹⁰B. Lengeler, W. R. Wampler, R. R. Bourassa, K. Mika, K. Wingerath, and W. Uelhoff, *Phys. Rev. B* 15, 49 (1977).

¹¹M. R. Halse, *Philos. Trans. R. Soc. London* 265, 507 (1969).

¹²D. K. Wagner and R. C. Albers, *J. Low Temp. Phys.* 20, 593 (1975).